Int. J. Electrochem. Sci., 14 **(2019)** 5386 – 5395, doi: 10.20964/2019.06.32

International Journal of
ELECTROCHEMICAL
SCIENCE
www.electrochemsci.org

Short Communication

Effect of Austenite Morphology on the Electrochemical Properties of Super Duplex Stainless UNS S 32750

Sanghyup Park, Byung-hyun Shin, Junghyun Park, Dohyung Kim, and Wonsub Chung[*]

Pusan National University, Department of Materials Science and Engineering, Busan, Korea
[*]E-mail: wschung1@pusan.ac.kr

Received: 11 February 2019 / *Accepted:* 1 April 2019 / *Published:* 10 May 2019

Volume fraction, Pitting resistance equivalent (PRE) as well as morphology of austenite on Duplex stainless steel can be changed through heat treatment by controlling annealing temperature and cooling rate. All specimens were evaluated for corrosion resistance according to shape of austenite phase after optimizing corrosion resistance as 5:5 volume fraction. The corrosion behavior was measured by the potentiodynamic polarization test and the pitting resistance was measured by Critical pitting temperature CPT. Austenite morphology increase corrosion current density on uniform corrosion without corrosion potential changing. The CPT of the specimen with the smallest grain boundary length of 2.3 μm/ μm^2 has the highest CPT as 76.3℃. Scanning Electron Microscopy showed that the pitting occurred in the grain boundary and propagated. It is confirmed that the reduction of the grain boundary length due to the control of the austenite morphology improve the pitting corrosion resistance of the UNS S 32750.

Keywords: Super duplex stainless steel; corrosion; Critical pitting temperature; Austenite Morphology; Grain boundary

1. INTRODUCTION

Stainless steel containing more than 11% chromium [1]. Added chromium and other alloys forming a passive layers on the surface and that have found widespread usage in many areas [2-4]. In particular, Duplex stainless steel(DSS), one of kind of stainless steel, has ferritic – austenitic microstructure and each ferrite phase and austenite phase in approximately same volume fraction [5-6]. DSS shows greater toughness and higher resistance to stress corrosion cracking and pitting corrosion to use in offshore plant and oil refining industry. DSS is qualified by Pitting Resistance Equivalent (PRE = wt. % Cr + 3.3 wt. % Mo + 16 wt. % N) for four types. The material used in this study is Super Duplex Stainless Steel(SDSS) with a PRE over then 40 and less than 50 [7].

Annealing temperature change the austenitic and ferritic phase volume fraction of SDSS [8]. When SDSS have nearly 50:50 fraction of austenitic and ferritic phase optimizing the corrosion

resistance [5]. Generally, usual stainless steel is carried out the Annealing at 1050 ° C[9]). SDSS is carried out heat treatment at 1100 ° C for equal PRE of austenite and ferrite [10]. Intermetallic precipitation or precipitation of secondary phase occurs during isothermal annealing [11]. Depending on the cooling rate conditions, sigma phase, chi phase, secondary austenite phase, etc. precipitate at a temperature near 700 - 900 ° C [12-13]. The precipitated secondary phase provides the pitting initiation site, decreasing resistance of pitting corrosion [14].

Previous research has analyzed the corrosion resistance after secondary phase precipitation or heat treatment under specific conditions. Nilsson analyzed the corrosion resistance of SDSS mainly by heat treatment temperature [15]. Chan analyzed the effects of secondary phase precipitation on the corrosion resistance in various temperature ranges were investigated [14]. In the literature observing changes in corrosion resistance depending on grain size, changes in grain size depending on the type of alloy may improve or reduce corrosion resistance. In the case of 304l austenitic stainless steel studied by Aghuy [16]. There is a possibility of pitting increases due to an increase in the length of the grain boundary, which does not mean an increase in the pitting potential. The existing literature has been only studying corrosion of super duplex stainless in various conditions of atmosphere and machining conditions [17-18]. However, there is no study on the effect of morphology on the pitting corrosion resistance of super duplex stainless to improve the corrosion resistance. To identify the effect of the morphology of super duplex stainless on the corrosion resistance, controlling the heat treatment condition and cooling rate is needed to optimize corrosion resistance by having 50:50 fraction of austenite and ferrite with the different morphology without other factors influence to corrosion resistance. By the study of controlling the morphology affected the corrosion resistance, may optimize the corrosion resistance of super duplex stainless. Thus, it could have a further increase of the corrosion resistance after optimizing corrosion resistance with 50:50 volume fraction of two phases by changing the heat treatment temperature and cooling time without changing the composition.

This study analyzed the effect of austenite morphology on the resistance of pitting when equivalent austenite, ferrite fraction and chemical composition were obtained after annealing with different temperature and cooling rate. The austenite morphology was analyzed by scanning electron microscope and optical microscope. Corrosion resistance was analyzed by the critical pitting temperature curve (Potentiostatic polarization curve) and potentiodynamic polarization curve.

2. MATERIALS AND METHODS

The Investigated material in this study was UNS S 32750 SDSS and the composition shown in Table 1.

Table 1. Chemical composition of commercial super duplex stainless steel UNS S 32750

Elements	C	N	Mn	Ni	Cr	Mo	Cu	W	PRE
Concentration (wt. %)	0.01	0.27	0.79	6.8	25.0	3.8	0.18	0.02	41.9

In this study every Pitting resistance equivalent (PRE = wt. % Cr + 3.3 wt. % Mo + 16 wt. % N) was calculated by this formula PRE of this material was calculated to be 42. Specimens were solution heat treated at various condition. The solution heat treatment temperatures and cooling rate for different austenite morphology experimented in this work were a) 1100°C by 5600 J/s, b)1200°C by 1.9 J/s, c) 1300°C by 5600 J/s 1200°C by 5600 J/s 1100°C by 5600 J/s respectively after annealing treatment 1h at every temperature. These heat treatment condition is shown in Table 2.

Table 2. Heat treatment condition to control austenite morphology of super duplex stainless steel UNS S 32750

Specimens	Conditions
a)	Heat treatment at 1100 ℃ 1h and quenching
b)	Heat treatment at 1200 ℃ 1h and air cooling
c)	Heat treatment at 1300 ℃ 1h ➔ 1200 ℃ 1h ➔ 1100 ℃ 1h each temperature respectively quenching

For the microscopic analysis, the samples after heat treatment were electrochemically etched by 10 wt. % NaOH solution at anodic potential of 6 V for 1 min. NaOH solution reveal austenite and ferrite phase to distinguish morphology of austenite. Before the etching all samples were grounded by SiC sandpapers from 80 to 2000 grit and grounded by 1 um diamond suspension. Field emission scanning electron microscopy (SEM, Hitachi S 4800) and optical microscope were used for Microstructure. Volume fraction of the UNS S 32750 was measured by ASTM E 1245 and concentration of chromium, nickel, molybden in austenite and ferrite was observed by energy dispersive X-ray spectroscopy(EDS) and concentration of nitrogen was calculated from reference [8].

All electrochemical measurements were carried out using Potentiometer (Versastat 4.0) with three-electrode cell containing pt mesh counter electrode and a saturated calomel electrode as reference electrode respectively. Prior to each test, the samples were successively wet ground by SiC sandpapers from 80 to 1200 grit rinsed with distilled water and dried by air compressor. In addition, Before electrochemical test, the open circuit potential was measured for 30 min, for steady state of specimens. Critical pitting temperature is measured by potentiostatic method, anodic potential of 700mV/$_{SCE}$ was applied in 5.84 Wt. % NaCl, and Increase solution temperature at a rate of 1 °C/min until current density increased over 100mA. Potentiodynamic polarization curve was acquired in 3.5wt% NaCl Solution. The range of potential was scanned from -0.3 to 1.2 V_{SCE} as 0.17mV/s of scan rate

3. RESULTS AND DISCUSSION

3.1 Effect of annealing temperature and cooling rate on austenite morphology

SDSS has a different Volume fraction, chemical composition depending on the Annealing temperature and cooling rate [19]. also, change the morphology of austenite. Figure 1. shows

morphology change on different annealing temperature and cooling rate brighter color phase is Austenite and darker color phase is ferrite. (a), fine ferrite was formed inside the austenite. (b) shows The austenite was coarsened and the ferrite inside the austenite decreased. formed a uniform austenite of 20 to 30μm. Micro ferrites of 3μm or less in the interior of austenite were lower than (a) normally when heated to 1200 degree ferrite is grow but due to the decreased cooling rate by air quenching volume fraction of austenite is increase and coarsen the austenite grain [17]. (c) Needle-shaped fine austenite of 3 um was formed between coarse austenite because it transformed in ferrite when it was heat-treated by the solidification.

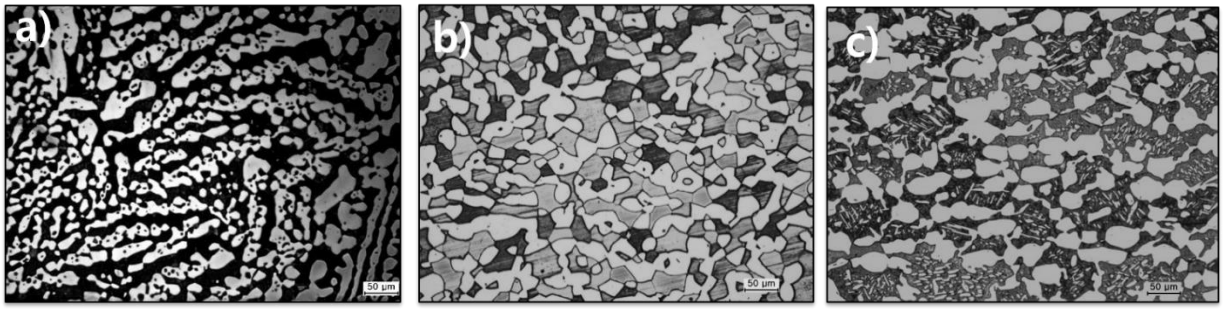

Figure 1. Microstructure with morphology of austenite on super duplex stainless steel UNS S 32750 a) Fine ferrite in austenite, b) Short length of grain boundary of austenite, c) Fine austenite between coarsened austenite

In case of c) 1300 degrees 1200 degrees and 1100 degrees, of temperature gave sufficient energy to grow. It has spherical shape to minimize energy because it had enough energy to spread austenite, and ferrite. It is characterized by the presence of austenite inside the ferrite as the area decreases. Also, No other secondary phase which can bad influence of pitting corrosion resistance has been found in a), b) c).

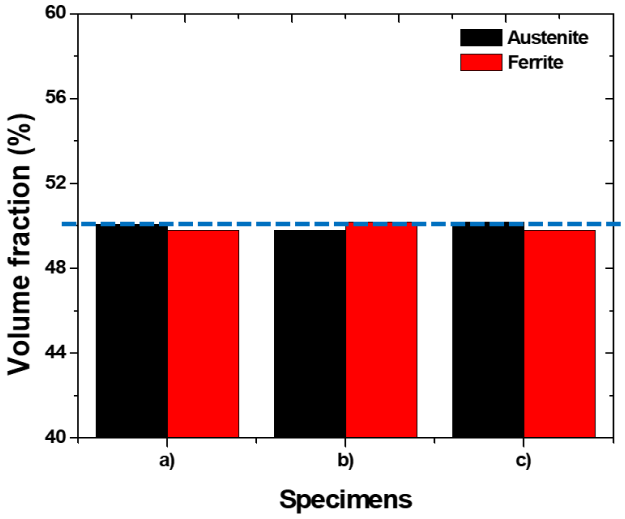

Figure 2. Volume fraction with austenite morphology of super duplex stainless UNS S 32750

The volume fraction of the test conditions had the equal fraction and that is showed at Fig 2. These showed the equal volume fraction. As the previous studies, same fraction has highest CPT [5].

Because the changed volume fraction changed the concentration of the main alloy in SDSS, the chemical composition was checked to check the PRE with morphology. Table 3 shows the composition of the main alloys according to the heat treatment conditions. That had equal Cr and Mo in austenite and ferrite. However, the content of Ni is found to be higher than the other conditions in austenite of (a). PRE is calculated as the composition of each phase [2, 20].

Table 3. Chemical composition with austenite morphology of super duplex stainless steel UNS S 32750

	Chemical composition (wt.%)					
Specimens	**Phase**	**Cr**	**Mo**	**Ni**	**N**	**Fe**
a)	**Austenite**	**23.6**	**3.2 ± 0.1**	**8.5 ± 0.2**	**0.48**	**Bal.**
	Ferrite	**25.7 ±**	**5.0 ± 0.1**	**5.9 ± 0.3**	**0.05**	
b)	**Austenite**	**23.8 ±**	**3.4 ± 0.1**	**8.0 ± 0.2**	**0.47**	
	Ferrite	**25.8 ±**	**4.8 ± 0.1**	**5.9 ± 0.2**	**0.05**	
c)	**Austenite**	**23.6 ±**	**3.4 ± 0.1**	**8.1 ± 0.1**	**0.47**	
	Ferrite	**26.3 ±**	**4.9 ± 0.1**	**5.8 ± 0.2**	**0.05**	

PRE with the heat treatment condition showed Figure 3. and the difference of PRE is 0.5. Because PRE is equal, CPT is highest.

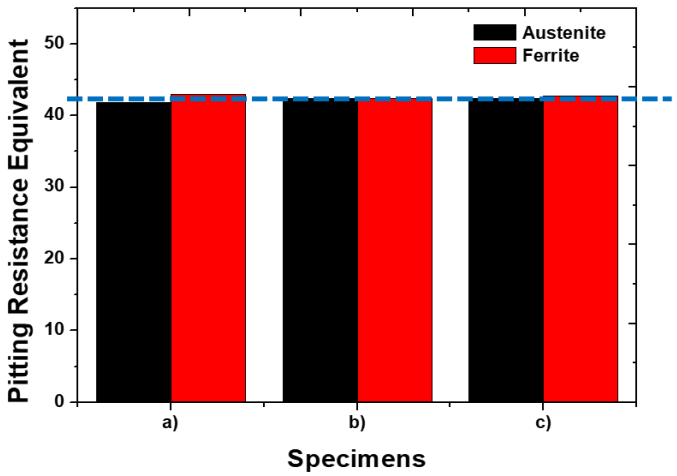

Figure 3. Pitting resistance equivalent number (PRE = wt. % Cr + 3.3 wt. % Mo + 16 wt. % N) with austenite morphology of super duplex stainless steel UNS S 32750

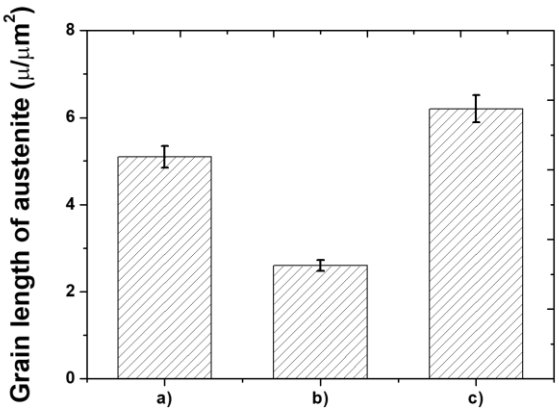

Figure 4. Grain length of austenite with different austenite morphology of super duplex stainless steel UNS S 32750

The morphology of austenite changed length of grain boundary and that showed at Figure 4. by image analyzer. This difference made by heat treatment. a) had 510 um/100um^2, b) had 260 um/100um^2, and c) had 620 um/cm^2. The needle types showed the highest length of the grain boundary and the fine ferrite showed the higher length more than the grain boundary of spherical shape.

The morphology with the heat treatment condition is checked and the morphology not made the difference the PRE due to the equal volume fraction. But austenite morphology change the length of grain boundary which had high energy, that is the factor to determine electrochemical properties [8].

3.2 Electrochemical analysis

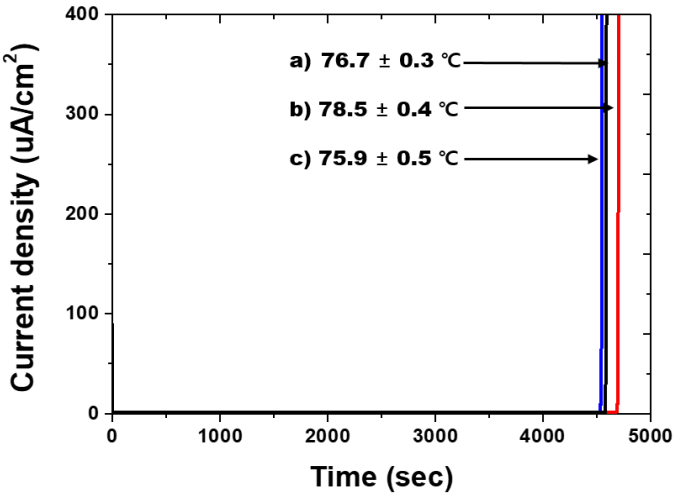

Figure 5. Critical pitting temperature curve(Potentiostatic curve) at 700 mV$_{SCE}$ in 5.85 wt. % NaCl of current density as function of time (temperature) with austenite morphology of super duplex stainless steel UNS S 32750

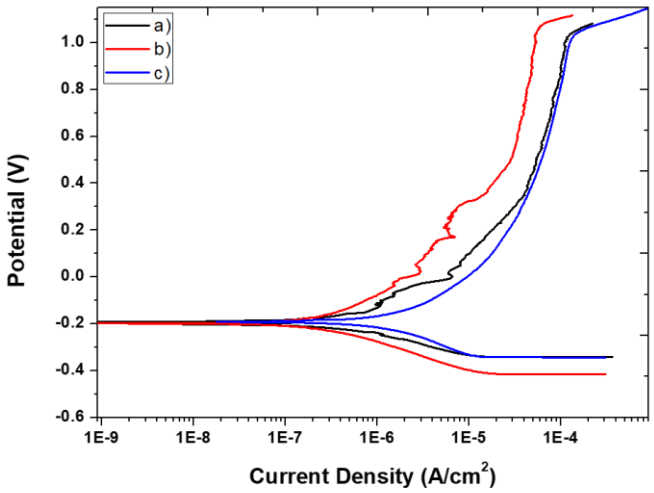

Figure 6. Potentiodynamic polarization curve in 3.5 wt. % NaCl with austenite morphology of super duplex stainless steel UNS S 32750 a) Fine ferrite in austenite, b) Short length of grain boundary of austenite, c) Fine austenite between coarsened austenite

The pitting corrosion of SDSS is measured to CPT by the change of current density with time. The increase of current density means the increase of surface by the pitting corrosion on base metal. Fig. 5 shows the CPT curve with specimen. These specimens had the equal PRE but CPT had the difference due to austenite morphology.

Table 4. Electrochemical parameter obtained by potentiodynamic curve with austenite morphology of super duplex stainless steel UNS S 32750 a) Fine ferrite in austenite, b) Short length of grain boundary of austenite, c) Fine austenite between coarsened austenite

Specimens	E_{CORR} (mV_{SCE})	I_{CORR} (nA/cm^2)	E_{PIT} (mV_{SCE})
a)	**- 198**	**421**	**1.033**
b)	**- 195**	**396**	**1.071**
c)	**- 193**	**2199**	**1.023**

Potentiodynamic polarization test is an experiment which can detect the overall corrosion behavior by changing the potential as function of the current density. The corrosion potential(E_{CORR}) and the corrosion current density(I_{CORR})can be known through the part where the slope changes abruptly in the area under the zonation polarization graph, and the pitting potential can be known through the point where the current suddenly increases after passivation. Fig 6. Shows the corrosion behavior with austenite morphology and Table 4 shows detail electrochemical parameter obtained from the potentiodynamic polarization curve. The corrosion potential had the equal value from -198 mV_{SCE} to –193 $mV_{SCE.}$ Because during the uniform corrosion, passive film still forms on the surface of the metal. But the corrosion current density had increased. It may caused by fine austenite and fine ferrite. By fine ferrite and austenite phase, grain boundary length become longer. Grain boundary has higher energy and

also has more defect than grain. Thus the defect region, grain boundary, has lower resistance to ion transfer since oxide grain boundary can have better ionic conductivities much larger than bulk oxide [21]. Therefore, higher conductivity may cause higher corrosion density. The active polarization curve shows the passivation and when that broken to the pitting corrosion, that made the pitting potential with austenite morphology. Because the pitting makes the increased surface, the potential and the current density is rapidly increased. Thus pitting corrosion potential is one of important factor of Pitting corrosion [22]. Pitting potential of each specimen are a) 1.033 V_{SCE}, b) 1.071V_{SCE} and c) 1.023V_{SCE} respectively. This pitting corrosion potential showed the same tendency compared with CPT [23].

3.3 Effect with austenite morphology on electrochemical properties of super duplex stainless steel UNS S 32750

Figure 7 show the pitting morphology with austenite morphology. The equal PRE of austenite and ferrite is checked at Fig. 4 and the pitting growth up to grain boundary of austenite [5]. When the PRE is equal, the grain boundary of austenite had the high dislocation and that worked the pitting site.

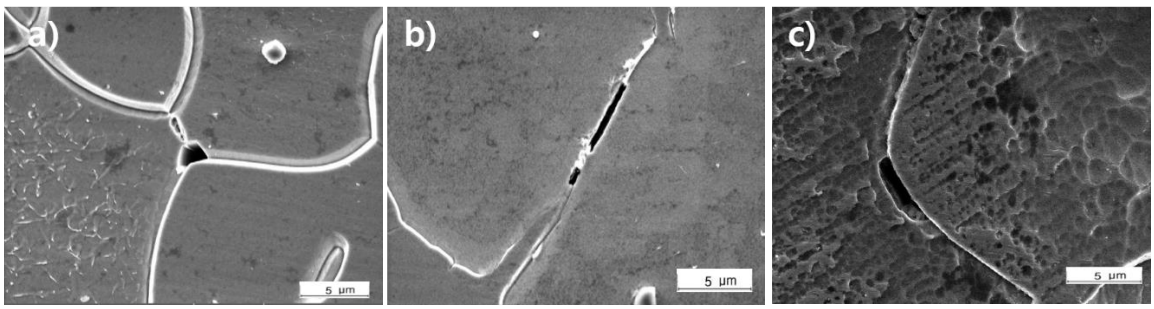

Figure 7. Pitting morphology with austenite morphology of super duplex stainless steel a) Fine ferrite in austenite, b) Short length of grain boundary of austenite, c) Fine austenite between coarsened austenite

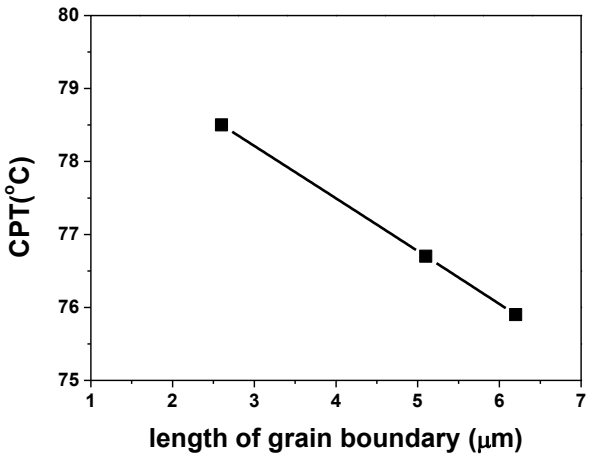

Figure 8. Critical pitting temperature as function of length of grain boundary of austenite on super duplex stainless steel UNS S 32750

The CPT is checked as function of the length of austenite grain boundary and that shows Fig. 8. The higher length decreased the CPT because that depends to the PRE and stable states. Fine austenite between coarsened austenite and fine ferrite in austenite work the decreasing the CPT and the increasing current density at active polarization.

4. CONCLUSIONS

The effects of austenite morphology on the electrochemical properties of UNS S32750 were studied to the potentiodynamic polarization curve and the critical pitting temperature and the following results were obtained.

Austenite morphology can be controlled by controlling Annealing temperature and cooling rate. The austenite morphology made the difference of electrochemical properties due to the change of the grain boundary on austenite. Effect of the austenite morphology is checked at pontentiodynamic polarization curve and the fine austenite and fine ferrite increased the current density at active polarization. That increased the corrosion rate of uniform corrosion. When the PRE and the volume fraction are equal, CPT test shows the effect of austenite morphology. The fine austenite and fine ferrite decreased the CPT due to the higher grain boundary. The increased grain boundary had the higher dislocation and the higher energy.

The electrochemical properties of SDSS need the control of austenite morphology to have the optimized corrosion resistance because the fine austenite and the fine ferrite decreased the corrosion resistance.

ACKNOWLEDGEMENTS
This research is supported by the Chung Mong-Koo Foundation.

References

1. G. Okamoto, *Corros. Sci.*, 13 (1973) 471
2. J. O Nilsson, *J. Mater. Sci. Technol.,* 8 (2013) 685
3. E. A. Lizloves, *Corrosion.*, 22 (1996) 279
4. M. annuzzi, A. Barnoush, R. Johnsen, npj *Materials Degradation*, 1 (2017) 2
5. H. Tan, Y. Jiang, B. Deng, T. Sun, J. Xu, J. Li, *Mater. Charact.*, 60 (2009) 1049
6. W. Zhang, J. Hu, *Mater. Charact.*, 79 (2013) 37
7. J. O. Nilsson, *Mater. Sci. Technol.*, 8 (1992) 685.
8. H. Y. Ha, M. H. Jang, T. H. Lee, J. Moon, *Mater. Charact.*, 106 (2015) 338
9. R. Jones, V. Randle, *J. Mater. Sci Eng* A., 527 (2010) 4275
10. S. T. kim, Y. S. Park, *Corros.*, 63 (2007) 114
11. T. Ishu, T. Ujiro, E. Hamada, S. Ishikawa, Y. Kato, *Journal of the Iron and Steel Institute of Japan.*, 97 (2011) 441
12. W. Zhang, D. N. Zou, G. W. Fan, J. Li, *Mater. Sci. Forum*, 620 (2009) 355
13. N. Llorca-Isern, H. López-Luque, I. López-Jiménez, M. V. Biezma, *Mater. Charact.*, 112 (2016) 20
14. K. Chan, S. Tjong, *Materials.*, 7 (2014) 5268

15. J. O. Nilsson, A. Wilson, *Mater. Sci. Technol.*, 9 (1993) 545
16. A. A. Aghuy, M. Zakeri, M. H. Moayed, M. Mazinani, *Corros. Sci.*, 94 (2015) 368
17. C. P. Meinhardt, A. Scheid, J. F. dos Santos, L. A. Bergmann, M. B. Favaro, C. E. F. Kwietniewski, *Mater. Sci. Eng., A*,706 (2017) 48
18. Z. Zhang, H. Zhao, H. Zhang, J. Hu, J. Jin, *Corros. Sci.*, 121 (2017) 22
19. B. H. Shin, S. Park, D. Kim, M. Hwang, W. Chung, *Int. J. Electrochem. Sci*., 14 (2019) 2430
20. B. H. Shin, J. Park, J. Jeon, S. B. Heo, W. Chung, *Anti-Corros. Methods* Mater., 65 (2018) 492
21. P. Marcus, V. Maurice, H. H. Strehblow, *Corros. Sci.*, *50* (2008) 2698
21. G. S. Frankel, *J. Electrochem. Soc., 145* (1998) 2186
22. X. Q. Xu, M. Zhao, Y. R. Feng, F. G. Li, X. Zhang, *Int. J. Electrochem. Sci*., *13* (2018) 4298